3476 *Chem. Mater.* **2009,** *21,* 3476–3478
DOI:10.1021/cm901265y

CHEMISTRY OF MATERIALS
Communication

Honeycomb Monolith-Structured Silica with Highly Ordered, Three-Dimensionally Interconnected Macroporous Walls

Jin-Woong Kim, Kohei Tazumi, Rika Okaji, and Masahiro Ohshima*

Department of Chemical Engineering, Kyoto University, Kyoto 615-8510, Japan

Received May 7, 2009
Revised Manuscript Received July 4, 2009

Velev et al.[1] were the first to report a unique method for preparation of highly ordered, three-dimensionally interconnected silica structures using a colloid crystal as a template. Since then, materials with ordered structures have been investigated intensively by many researchers over the past decade.[1−10] The unique structure reported by Velev's group was determined by Zakhidov et al. to be an inverse opal.[2] The resulting 3D structures have great potential as photonic crystals, catalysts, electrodes, and biomaterials.[11,12] Several methods, such as filtration,[1,3,4] centrifugation,[13] and drying,[5] have been proposed for fabricating the regularly aligned colloid crystals. Infiltration of an inorganic precursor into a prearranged template has often been used to prepare the inverse opal structure.[1−4] Recently, a new method was developed, involving direct introduction of colloid particles into precursor solutions.[8,9] Iskandar et al.[8] prepared a reverse opal structure from silica by dip coating a colloidal suspension of SiO_2 and polystyrene latex (PSL) mixture without preordered arrangement of PSL. Oh et al.[9] conducted a sol−gel synthesis of the mesoporous silicate in the presence of the polymer latex. However, these methods do not provide materials of large size and uniform structure. More development is necessary to discover a simple method for preparation of relatively large structures for commercial applications, such as catalysts and adsorbents.

Herein, we show that unidirectional freezing of a colloidal suspension composed of two kinds of monodispersed nanoparticles is a simple method for producing a honeycomb monolith structure with highly ordered, three-dimensionally interconnected macroporous walls. Unidirectional freezing is a relatively simple and cost-effective method for the creation of microhoneycomb monolith structures from various kinds of materials, such as ceramics,[14] polymers,[15,16] and carbon.[17] This method results in an aligned, porous structure with smooth-walled or ladder-like-walled microscale tubes aligned along the freezing direction, as well as a honeycomb structure in the cross-section. This structure has great potential as a catalyst support,[18] catalyst,[19] substrate for drug delivery,[20] or bioscaffold[21] due to its inherently high contact efficiency and the controllability of its unique morphology. The unidirectional freezing method has been applied to several systems, including sol−gel[22] and polymer−solvent systems,[15,16] where a solid−liquid phase separation can be induced by lowering the temperature. The resulting solid phase can be utilized as a template. The liquid phase is later solidified in the template by reaction, solvent evaporation, or binder materials. However, there have been no applications of this method to prepare a highly ordered and three-dimensionally interconnected structure by adopting the particle templating technique.

Silica sol and monodispersed poly[styrene-(*co*-2-hydroxyethyl methacrylate)] (PSHEMA) latex were used for this study. Silica sol (Snowtex OS) was kindly supplied by Nissan Chemical Industries Co., Ltd. The diameter of the silica nanoparticles was in the range of 8−11 nm. Monodispersed PSHEMA latex was prepared by extending the Reese and Asher's procedure.[23] The details of the preparation method are described in the Supporting Information. As shown in Figure S1 (Supporting Information), spherical PSHEMA particles with uniform diameter were obtained. The average particle diameter of PSHEMA decreased with an increase of the content of sodium dodecyl sulfate. PSHEMA particles with an average diameter of 385 nm and a CV value of 2.86% were used for this study. The dried

(1) Velev, O. D.; Jede, T. A.; Lobo, R. F.; Lenhoff, A. M. *Nature* **1997**, *389*, 447.
(2) Zakhidov, A. A.; Baughman, R. H.; Iqbal, Z.; Cui, C. X.; Khayrullin, I.; Dantas, S. O.; Marti, I.; Ralchenko, V. G. *Science* **1998**, *282*, 897.
(3) Park, S. H.; Xia, Y. N. *Adv. Mater.* **1998**, *10*, 1045.
(4) Holland, B. T.; Blanford, C. F.; Stein, A. *Science* **1998**, *281*, 538.
(5) Yang, P. D.; Deng, T.; Zhao, D. Y.; Feng, P. Y.; Pine, D.; Chmelka, B. F.; Whitesides, G. M.; Stucky, G. D. *Science* **1998**, *282*, 2244.
(6) Iskandar, F.; Mikrajuddin; Okuyama, K. *Nano Lett.* **2001**, *1*, 231.
(7) Iskandar, F.; Mikrajuddin; Okuyama, K. *Nano Lett.* **2002**, *2*, 389.
(8) Iskandar, F.; Abdullah, M.; Yoden, H.; Okuyama, K. *J. Appl. Phys.* **2003**, *93*, 9237.
(9) Oh, C. G.; Baek, Y. Y.; Ihm, S. K. *Adv. Mater.* **2005**, *17*, 270.
(10) Woo, S. W.; Dokko, K.; Sasajima, K.; Takei, T.; Kanamura, K. *Chem. Commun.* **2006**, 4099.
(11) Stein, A.; Schroden, R. C. *Curr. Opin. Solid State Mater. Sci.* **2001**, *5*, 553.
(12) Yuan, Z. Y.; Su, B. L. *J. Mater. Chem.* **2006**, *16*, 663.
(13) Wijnhoven, J.; Vos, W. L. *Science* **1998**, *281*, 802.
(14) Fukasawa, T.; Ando, M.; Ohji, T.; Kanzaki, S. *J. Am. Ceram. Soc.* **2001**, *84*, 230.
(15) Zhang, H. F.; Hussain, I.; Brust, M.; Butler, M. F.; Rannard, S. P.; Cooper, A. I. *Nat. Mater.* **2005**, *4*, 787.
(16) Kim, J.-W.; Taki, K.; Nagamine, S.; Ohshima, M. *Chem. Eng. Sci.* **2008**, *63*, 3858.
(17) Mukai, S. R.; Nishihara, H.; Yoshida, T.; Taniguchi, K.; Tamon, H. *Carbon* **2005**, *43*, 1563.
(18) Nishihara, H.; Mukai, S. R.; Tamon, H. *Carbon* **2004**, *42*, 899.
(19) Mukai, S. R.; Nishihara, H.; Shichi, S.; Tamon, H. *Chem. Mater.* **2004**, *16*, 4987.
(20) Gutierrez, M. C.; Garcia-Carvajal, Z. Y.; Jobbagy, M.; Rubio, T.; Yuste, L.; Rojo, F.; Ferrer, M. L.; del Monte, F. *Adv. Funct. Mater.* **2007**, *17*, 3505.
(21) Ma, P. X.; Zhang, R. Y. *J. Biomed. Mater. Res.* **2001**, *56*, 469.
(22) Nishihara, H.; Mukai, S. R.; Yamashita, D.; Tamon, H. *Chem. Mater.* **2005**, *17*, 683.
(23) Reese, C. E.; Asher, S. A. *J. Colloid Interface Sci.* **2002**, *248*, 41.

 Published on Web 07/09/2009

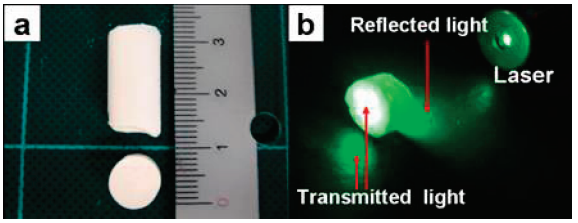

Figure 1. Photographs of honeycomb monolith-structured silica: (a) overall image of the calcined sample and (b) the result of laser irradiation perpendicular to the freezing direction.

PSHEMA particles were added to the silica sol with a 74.2/25.8 PSHEMA/silica volume ratio. The PSHEMA particles were dispersed by stirring and ultrasonic treatment. After dispersion treatment, the colloidal solution was poured into a polypropylene (PP) test tube, 100 mm in length and 10 mm in diameter. The test tube was then frozen unidirectionally by immersion into a liquid nitrogen bath at a constant rate. After freezing the solution completely, the solidified sample was freeze-dried at 268 K for 4 days. The freeze-dried sample was then calcined at 723 K to remove PSHEMA particles. The morphologies of the resulting porous samples were observed by scanning electron microscopy (SEM; Tiny-SEM 1540, Technex Lab Co. Ltd.). In the unidirectional freezing process, the freezing rate changes until a pseudo-steady state is established. Tamon and co-researchers[18,22] suggested that the pseudo-steady state of ice growth is established at least 5 cm above the bottom of the tube. Because of this, we harvested a sample from 5 cm above the bottom of the tube for SEM observation.

Figure 1a shows a photographic image of calcined honeycomb monolith-structured silica, several centimeters in length and about 8 mm in diameter. The test results for laser transmission perpendicular and vertical to the freezing direction are illustrated in Figure 1b and Figure S2c (Supporting Information), respectively. When the laser is perpendicular to the freezing direction, the strength of transmitted light is strongest in the center area, and some light is transmitted through the sidewall because the porous structure has highly ordered, three-dimensionally interconnected macroporous walls. The strength of the light transmitted vertical to the freezing direction was weaker than the strength of the light transmitted perpendicular to the freezing direction.

Figure 2 shows typical SEM micrographs of prepared silica microscale honeycomb structures. The SEM sample was prepared from PSHEMA/silica sol with a 20 vol % total particle concentration, a 74.2/25.8 PSHEMA/silica volume ratio, and a 3.5 cm h^{-1} immersion rate. Figure 2a, b shows SEM micrographs of cross-sectional areas of the sample, cut parallel and perpendicular to the freezing direction, respectively. Both images clearly show a honeycomb monolith structure in the cross section, with smooth-walled microtubes aligned along the freezing direction. The magnified SEM micrographs of the cross-sectional area parallel to the freezing direction are shown in Figure 2c. Macropores can be observed on the walls of the silica honeycomb monolith structure. The pores originated from PSHEMA and were well aligned in

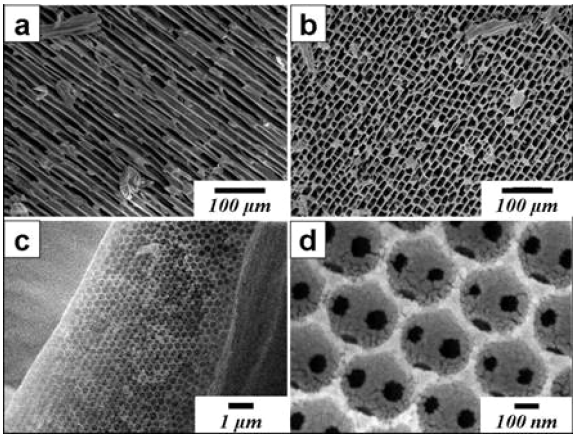

Figure 2. Micrographs of honeycomb monolith structures prepared from PSHEMA/silica sol with a 20 vol % total particle concentration, a 74.2/25.8 PSHEMA/silica volume ratio, and a 3.5 cm h^{-1} immersion rate. (a) Cross-sectional area parallel to the freezing direction, (b) cross-sectional area perpendicular to the freezing direction, (c) magnified cross-sectional area parallel to the freezing direction, and (d) magnified micrograph that shows interconnected macropores prepared by calcination.

three dimensions. This result indicates the spontaneous alignment and packing of two particles with different sizes occurring during the unidirectional freezing process. Figure 2d clearly shows that the walls have highly ordered, three-dimensionally interconnected macropores. The macropore size was determined by the size of the PSHEMA particles. The size of the macropores is about 300 nm, which is smaller than the particle size due to shrinkage during calcination. N_2 adsorption−desorption isotherms of this sample at 77 K were measured to confirm the existence of mesopores. The BET surface area was 281 m^2 g^{-1}. The pore size distribution analysis showed that this sample has a clear peak at 3.6 nm (Figures S3 and S4, Supporting Information).

The schematic diagram of the fabricated structure is illustrated in Scheme 1. The structure has three different kinds of pores: microscale channels prepared by templating ice crystals, highly ordered and three-dimensionally interconnected macropores prepared by templating PSHEMA particles, and mesopores between silica particles. The average diameter of the microscale channels and the wall thicknesses can be controlled by the freezing rate and total particle concentration. The test results are shown in Figures S5 and S6 (Supporting Information). The effects of the freezing rate and the total particle concentration on the microscale channel diameter and the wall thickness were investigated using SEM micrographs and mercury porosimetry. The average microscale channel diameter decreased with an increase in the freezing rate and total particle concentration. The average wall thickness decreased with an increase in freezing rate and a decrease in total particle concentration (Figures S7−9, Supporting Information).

In a previous study,[16] we created a honeycomb monolith structure from polylactic acid (PLA) and a dehydrated 1,4-dioxane solution, where the 1,4-dioxane crystalline structure was used as a template. The solvent was crystallized, and the crystals grew in the freezing direction under

Scheme 1. Schematic Diagram of the Fabricated Structure[a]

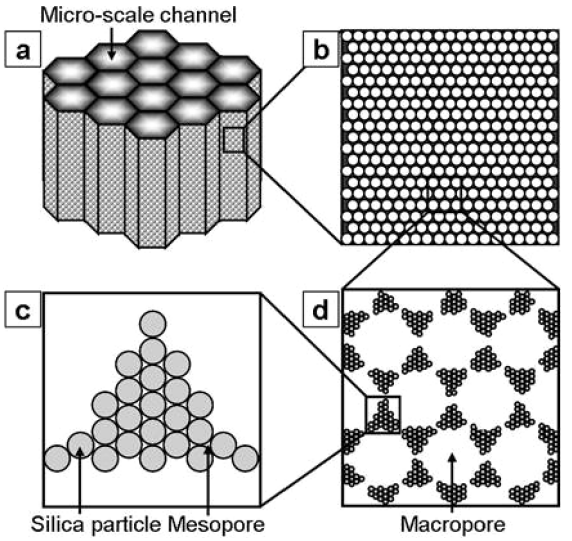

[a] **(a) Honeycomb monolith structure, (b) highly ordered macropores, (c) magnified macropores interconnected three dimensionally to each other, and (d) packed silica particles.**

the constitutional supercooling condition. Thus, the crystal growth followed the Mullins-Sekerka instability theory.[24] Impurities in the solution increase instability and enhance transition from a cellular to a dendritic structure in solvent crystals. However, in the colloidal solution used in the present work, the existence of particles in the freezing solution did not seem to change the degree of constitutional supercooling and instability. Therefore, the creation of smooth-walled (cellular type) microscale tubes was not hindered by the particles. The speculated mechanism of particle packing and self-organization in the ice template is illustrated in Scheme 2. In the course of unidirectional crystal growth of water, the particles are expelled from the growing ice crystals.[15,25] The concentration of water in the colloidal liquid phase surrounded by ice is gradually decreased according to the growth of the ice. On the other hand, the particle density in the colloidal liquid phase increases while maintaining dispersion, and finally, the particles are closely packed. The growth rate of the ice crystals could be considered to affect the repulsion

(24) Mullins, W. W.; Sekerka, R. F. *J. Appl. Phys.* **1964**, *35*, 444.
(25) Asthana, R.; Tewari, S. N. *J. Mater. Sci.* **1993**, *28*, 5414.

Scheme 2. Schematic Diagram Explaining Particle Packing by the Unidirectional Growth of Ice Crystals

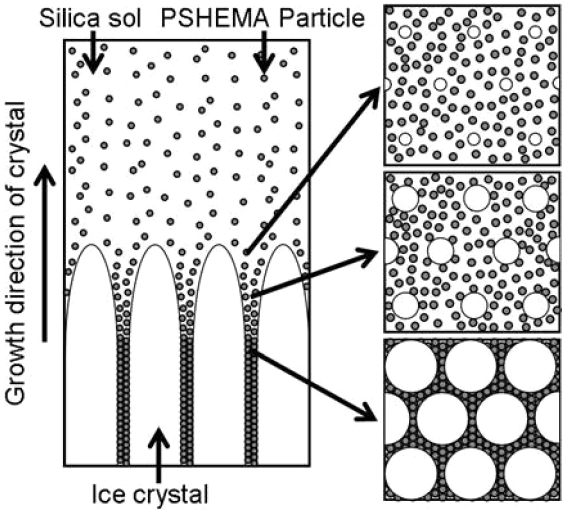

of particles and the ordered arrangement of PSHEMA/silica particles.

In conclusion, the unidirectional freezing scheme is proposed as a simple method for packing colloidal silica and preparing honeycomb monolith-structured silica with highly ordered, three-dimensionally interconnected macroporous walls. The relatively large size inverse opal structure, which has aligned microscale channels, can be easily produced using this method. The experimental results indicate that three-dimensionally interconnected macroporous structures develop by spontaneous self-organization of two kinds of particles in the growing ice template. This new method could be applied to a range of nanoparticle suspensions for particle packing and colloidal crystal preparation. We expect potential applications in a wide range of areas, such as catalysts, adsorbents, tissue scaffolds, ultralightweight materials, and microfluidics.

Supporting Information Available: Detailed preparation method of monodispersed PSHEMA particles, laser transmission test results, SEM micrographs of samples, nitrogen isotherms, results of mercury porosimetry measurements, and graphs that illustrate the effects of the immersion rate and total particle concentration on the average diameter of the microscale channels and the wall thicknesses (PDF). This material is available free of charge via the Internet at http://pubs.acs.org.